IOP Publishing Physica Scripta
Phys. Scr. 95 (2020) 045201 (8pp) https://doi.org/10.1088/1402-4896/ab5a36

Numerical study on enhancement of heat transfer in hybrid nano-micropolar fluid

Shafia Rana[1], M Nawaz[1], Salman Saleem[2] and Sayer Obaid Alharbi[3]

[1] Department of Applied Mathematics & Statistics, Institute of Space Technology, Islamabad, 44000, Pakistan
[2] Department of Mathematics, College of Science, King Khalid University, Abha 61413, Saudi Arabia
[3] Mathematics Department, College of Science Al-ZulÖ, Majmaah University, Majmaah 11952, Saudi Arabia

E-mail: nawaz_d2006@yahoo.com

Received 2 June 2019, revised 12 November 2019
Accepted for publication 21 November 2019
Published 11 February 2020

Abstract

Hybrid nanoparticles correlations together with governing models for the flow of micropolar fluid are used to develop novel complex coupled nonlinear set of differential equations. The solutions are computed by using the finite element method (FEM) and results are validated after convergence and grid-free analysis. The macroscopic velocity and micro-rotation field are investigated versus parametric variation. The temperature field is examined for various emerging dimensionless parameters. A significant improvement in the thermal performance of micropolar fluid due to simultaneous dispersion of Cu and Al_2O_3 (hybrid nanoparticles) is noted. Therefore, simultaneous dispersion of Cu and Al_2O_3 for significant improvement in thermal performance of micropolar fluid is recommended rather the dispersion of copper nanoparticles. Surprisingly micro rotation field for nano micropolar mixture near the vicinity of the wall is less than the micro-rotation field for hybrid nano-micropolar fluid. However, away from the wall opposite dynamics for the micro-rotation field are observed.

Keywords: micro-rotation, hybrid nanofluid, micropolar fluid, couple stress, wall heat flux

(Some figures may appear in colour only in the online journal)

1. Introduction

Enhancement of the thermal performance of working fluids by dispersion of nanoparticles has attracted as extensive scientific attention as it is proven fact that dispersion of nanoparticles optimizes the effective thermal conductivity of the fluid to which these nano-sized particles are dispersed. Experimental and theoretical studies show that working pure fluids have relatively poor heat transfer characteristics than those for fluid containing nanoparticles. Remarkable enhancement in thermal performance of mixture containing nano-sized metallic particles has been observed. Since from the pioneering work of Choi [1], many researchers have conducted numerical and experimental studies from different aspects regarding the advantages of the use of nanoparticles in thermal design and related applications. However, some latest and the most related studies are being described. For example, Dogonchi *et al* [2] studied the role of dispersion of Fe_3O_4 on enhancement of heat transfer in water in a container by using control volume finite element method (FEM). They investigated the effects of thermal radiations and the role of nanoparticles on drug delivery during medical treatment of cancer. Dogonchi and Hashim [3] investigated the impact of Fe_3O_4 in water flowing in circular cylinder. They also discussed flow in a container like a rhombus. They performed various control volume finite element experiments to analyzed the impact of magnetic field dependent viscosity on the transport of heat in a nanofluid. Sheikholeslami *et al* [4] modeled transport of phenomenon in Darcian medium exposed to the magnetic field and solved the mathematical models using control volume FEM in order to investigate the impact of nanoparticles on the transport of heat in the water. Sheikholeslami and Rokni [5] discussed the influence coulomb force on the transport of heat in nanofluid in an enclosure exposed to thermal radiations. Sheikholeslami and Ghasemi [6] numerically studied stratification phenomenon during heat transfer in

a nanofluid emitting thermal radiations. Sheikholeslami *et al* [7] studied heat transfer in a heat storage unit containing nanofluid. They also studied the role of fins on heat transfer through fins with heat exchanger. Sheikholeslami *et al* [8] have simulated melting of PCM by means of finite volume approach. Sheikholeslami *et al* [9] also studied heat transfer augmentation and energy loss inside a pipe equipped with innovator turbulators. Safaei *et al* [10] developed mathematical models for the role of hybrid nanoparticles ($CoFe_2O_4$ and SiO_2) on the transfer of heat in a liquid contained by a permeable medium exposed to applied magnetic and solved the modeled problems by using LBM numerical scheme to explored the effects of arising parameters on transfer heat. Safaei *et al* [11] analyzed the impact of ZnO–TiO on the thermal conductivity of ethylene glycol by using artificial network approach by interpolating the experimental data. Nadeem *et al* [12] numerically studied the influence of free stream velocity on heat transfer in a mixture of water containing Cu and Al_2O_3 while their transportation in a circular cylinder subjected to thermal slip mechanism. Nadeem *et al* [13] numerically studied the effects of hybrid nanoparticles and heat generation/absorption in fluid over convectively heat surface in the rotating frame of reference. Iqbal *et al* [14] discussed an enhancement in thermal performance of water subjected to the dispersion of hybrid nanoparticles (Cu and CuO). Sheikholeslami *et al* [15] investigated simultaneous by the impact of variable magnetic field and magnetization of hybrid nanoparticles on heat transport in a liquid in a circular cavity by using the FEM. Nadeem and Abbas [16] developed mathematical problems for simultaneous effects of boundary slip, free stream velocity and hybrid nanosized particles on the transport of heat in a dusty micropolar fluid having CuO and Al_2O_3 experiencing porous medium resistance. Das *et al* [17] considered dispersion of Cu and Al_2O_3 nanostructures in water simultaneously and performed theoretical analysis in the presence of entropy generation. They noticed a significant rise in thermal conductivity of water mixture containing hybrid nanoparticles (Cu, Al_2O_3) Taslimah *et al* [18] developed heat transfer models for Blasius flow of water containing Cu and Al_2O_3 as hybrid nano-structures and solved the modeled problems in order to investigate thermal performance of the hybrid nanofluid. In this work, they have observed that the Nusselt number for the case of blade shaped nanoparticles is greater than the Nusselt number for the case of platelets cylindrical, brick and spherical shaped nanoparticles. Makinde *et al* [19] performed mathematical modeling for simultaneous effects of nonlinear thermal radiation, magnetic field and melting heat transfer phenomenon of wall on the transportation of heat energy in micropolar fluid over moving surface. Sheikholeslami *et al* [20] studied the impact of magnetic field on the transport of heat in fluid containing nanoparticles numerically using Runge–Kutta method and observed a noteable enhancement in the transfer of heat due to dispersion of nanoparticles. Saleem *et al* [21] performed an optimal analysis for the influence of viscous dissipation and heat source in nano-material exposed thermal radiations. Adil *et al* [22] carried out numerical simulations for flow of micropolar fluid exposed magnetic field and dispersion of nanoparticles.

Present study has uses micropolar theory proposed by Eringin [23]. Example of micropolar fluids are suspensions, ferrofluids, blood, bubbly liquids, liquid crystals etc. Eringin's theory of micropolar fluid is based on continuum hypothesis and it states that micropolar fluids are those which consist of rigid, randomly oriented or spherical particles (suspended in a viscous medium) with their own spins and microrotations. For flow modeling of micropolar fluids, an additional conservation law 'the law of conservation of angular momentum' is need. As proposed by Eringin, this theory is not molecular theory rather than macroscopic/continuum and considers microrotation of spherical structures immersed in viscous fluid macroscopically. The micropolar liquids containing micro-structures exhibit non-Newtonian rheology which is described by an additional conservation law (the law of conservation of angular momentum) with usual conservation laws. On the other hand, there are two types of deformations (i) macro-motion governed by conservation of linear momentum and (ii) the microrotation governed by the law of conservation of angular momentum. These two types of motions are characterized by two types of stress-strain relations. The fluid with solid micro-structures are called micropolar fluid and these constitutive equations are proposed by Eringin [23]. Later on, several researches on the micropolar fluid were conducted. However, some recent studies on the micropolar fluid are of great importance and are mentioned through [24–27].

Through literature review, the author came to know that the numerical study (using FEM) on the impact of hybrid nanoparticles on the thermal performance of polymers containing micro-structures (such fluids are called micropolar fluid) has not been conduct so far. This work will fill this space in the existing scientific developments. The developed mathematical models are solved by FEM which is powerful technique and has ability of catering with the complexity and nonlinearities in the problems. After convergence, grid independence and verification of results, the parametric investigation is carried out through numerical experiments. The simulations obtained during the numerical experiments are displayed and discussed in the results and discussion section. Finally, the results are briefly described.

2. Physical arrangements

Let us investigate the improvement in thermal performance of micropolar fluid over an elastic body moving with velocity $U_w(x) = ax$ and subjected to the dispersion of hybrid nanoparticles Cu and Al_2O_3. The stretchable body is electrically nonconducting and is hot such that $T_w(x) > T$ of micropolar fluid, is exposed to magnetic field [0, B_0Ax^{-1}, 0]. The wall temperature $T_w(x)$ is varying as $T_w(x) = T_\infty + dT_0x^2$. Schematic representation is given by Figure 1.

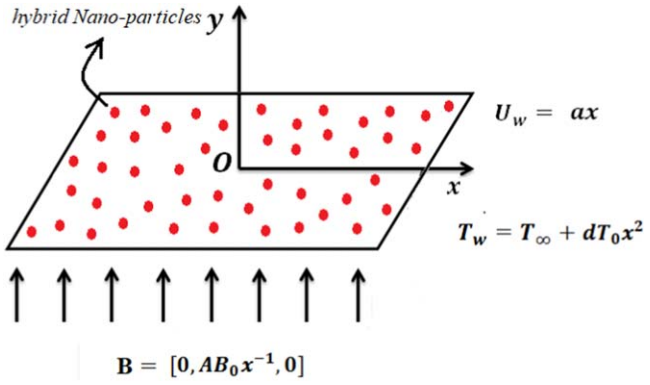

Figure 1. Geometry of the problem and coordinates system.

Two dimensional mass, momentum and energy equations are

$$\frac{\partial u}{\partial x} + \frac{\partial v}{\partial y} = 0, \tag{1}$$

$$u\frac{\partial u}{\partial x} + v\frac{\partial u}{\partial y} = \frac{1}{\rho_{hnf}}(\mu_{hnf} + \lambda_{hnf})\frac{\partial^2 u}{\partial y^2} - \frac{\lambda_{hnf}}{\rho_{hnf}}\frac{\partial N}{\partial y} - \frac{\sigma_{hnf}A^2B_0^2x^{-2}u}{\rho_{hnf}}, \tag{2}$$

$$\rho_{hnf}j\left(u\frac{\partial N}{\partial x} + v\frac{\partial N}{\partial y}\right) = \gamma_{hnf}\frac{\partial^2 N}{\partial y^2} - \lambda_{hnf}(2N + \frac{\partial u}{\partial y}), \tag{3}$$

$$(\rho c_p)_{hnf}\left(u\frac{\partial T}{\partial x} + v\frac{\partial T}{\partial y}\right) = k_{hnf}\frac{\partial^2 T}{\partial y^2} + \sigma_{hnf}A^2B_0^2x^{-2}u^2 + \left[\mu_{hnf} + \frac{\lambda_{hnf}}{2}\right]\left(\frac{\partial u}{\partial y}\right)^2 + \frac{\lambda_{hnf}}{2}\left(\frac{\partial u}{\partial y} - 2N\right)^2 + (\alpha + \beta + \gamma)\left(\frac{\partial N}{\partial y}\right)^2, \tag{4}$$

where $[u, v]$ are the velocity, T is the temperature of the fluid, $K = \lambda_f/\mu_f$ is the micropolar parameter, $j = (\nu_{hnf}/a)$, j is taken as length scale, B_0 is magnetic induction, A, d, a are consistency parameters, α, β, γ are the material parameters and $\gamma_{hnf} = (\mu_{hnf} + \lambda_{hnf}/2)j = \mu_{hnf}(1 + K/2)j$, γ_{hnf} is the spin gradient viscosity of hybrid nanofluid and is assumed to be constant.

The initial and boundary conditions are

$$\begin{aligned} &u(x, y) = U_w(x),\ v = 0,\ T = T_w,\\ &N(x, y) = -n\frac{\partial u}{\partial y} \text{ at } y = 0,\\ &u \to 0,\ T \to T_\infty,\ N(x, y) \to 0, \text{ as } y \to \infty. \end{aligned} \tag{5}$$

where n $(0 \leqslant n \leqslant 1)$ is a constant. Further, $n = 0$ is the case when micro-motion vanishes at the surface and $n = 0.5$ is the case when micro-motion does not vanishes at the solid surface. However, $n = 1$ is the case of turbulent flow which is not the case of present study.

By using new variables

$$\begin{aligned} &u = \frac{\partial \psi}{\partial y},\ v = -\frac{\partial \psi}{\partial x},\ \psi(x, y) = \sqrt{a\nu_f}xf(\eta),\\ &\theta(\eta) = \frac{T - T_\infty}{T_w - T_\infty},\ \eta = \sqrt{\frac{a}{\nu_f}}y,\ N = \frac{a^{3/2}x}{\sqrt{\nu_f}}g(\eta), \end{aligned} \tag{6}$$

in equation (6) into (1)–(5), one gets

$$\left.\begin{aligned} &(1 + K)f''' + Kg' + \frac{\sigma_{hnf}}{\sigma_f\left[(1 - \varphi_2)\left\{1 - \varphi_1 + \varphi_1\frac{\rho_{s1}}{\rho_f}\right\} + \varphi_2\frac{\rho_{s2}}{\rho_f}\right]}Haf' - (1 - \varphi_1)^{2.5}(1 - \varphi_2)^{2.5}\\ &\left[(1 - \varphi_2)\left\{1 - \varphi_1 + \varphi_1\frac{\rho_{s1}}{\rho_f}\right\} + \varphi_2\frac{\rho_{s2}}{\rho_f}\right][f'^2 - ff''] = 0\\ &f(0) = 0, f'(0) = 1, f'(\infty) = 0 \end{aligned}\right\}, \tag{7}$$

$$\left.\begin{aligned} &\left(1 + \frac{K}{2}\right)g'' - K[2g + f''] - (1 - \varphi_1)^{2.5}(1 - \varphi_2)^{2.5}\\ &\left[(1 - \varphi_2)\left\{1 - \varphi_1 + \varphi_1\frac{\rho_{s1}}{\rho_f}\right\} + \varphi_2\frac{\rho_{s2}}{\rho_f}\right][f'g - fg'] = 0\\ &g'(0) = -nf''(0),\ g'(\infty) = 0 \end{aligned}\right\}, \tag{8}$$

$$\left.\begin{aligned} &\frac{k_{hnf}}{k_f}\theta'' + \frac{\sigma_{hnf}}{\sigma_f}HaPr\ Ecf'^2 + \left(1 + \frac{K}{2}\right)\frac{EcPr}{(1 - \varphi_1)^{2.5}(1 - \varphi_2)^{2.5}}f''^2\\ &+\frac{K}{2}\frac{Pr\ Ec}{(1 - \varphi_1)^{2.5}(1 - \varphi_2)^{2.5}}[f''^2 + 4g^2 - 4gf''] + CPr\ Ec\ Reg'^2\\ &+Pr\left[(1 - \varphi_2)\left\{1 - \varphi_1 + \varphi_1\frac{(\rho c_p)_{s1}}{(\rho c_p)_f}\right\} + \varphi_2\frac{(\rho c_p)_{s2}}{(\rho c_p)_f}\right][f\theta' - f'\theta] = 0\\ &\theta(0) = 1,\ \theta(\infty) = 0 \end{aligned}\right\}, \tag{9}$$

where Hartmann number (Ha), Prandtl number (Pr), Eckert number (Ec), Reynold number (Re) and the dimensionless material parameter (C) are expressed by

$$Ha = \frac{\sigma_f A^2 B_0^2 x^2}{a\rho_f},\ Pr = \frac{\mu_f (c_p)_f}{k_f},\ Ec = \frac{(ax)^2}{(c_p)_f (T_w - T_\infty)},$$

$$Re = \frac{ax^2}{\nu_f},\ C = \frac{\alpha + \beta + \gamma}{\mu_f x^2}.$$

The wall shear stress [28, 29] is defined by

$$C_f = \frac{(\mu_{hnf} + \lambda_{hnf})\frac{\partial u}{\partial y} + \lambda_{hnf} N\Big|_{y=0}}{\rho_f (U_w)^2} = \frac{(1 + K/2)}{\sqrt{Re}\,(1-\varphi_1)^{2.5}(1-\varphi_2)^{2.5}} f''(0), \tag{10}$$

The wall couple stress is defined by

$$C_g = \frac{x\gamma_{hnf}\frac{\partial N}{\partial y}\Big|_{y=0}}{\rho_f (U_w)^2} = \frac{\left(1 + \frac{K}{2}\right)}{\sqrt{Re}\,(1-\varphi_1)^{2.5}(1-\varphi_2)^{2.5}} g'(0), \tag{11}$$

The wall heat flux is given by

$$Nu = -\frac{xk_{hnf}\frac{\partial T}{\partial y}\Big|_{y=0}}{k_f (T_w - T_\infty)} = -\sqrt{Re}\frac{k_{hnf}}{k_f}\theta'(0). \tag{12}$$

Thermo-physical properties appearing in equations (7)–(12) are correlated by the following models

$$\frac{\rho_{hnf}}{\rho_f} = (1-\varphi_2)\left\{1 - \varphi_1 + \varphi_1\frac{\rho_{s_1}}{\rho_f}\right\} + \varphi_2\frac{\rho_{s_2}}{\rho_f},$$

$$\frac{(\rho c_p)_{hnf}}{(\rho c_p)_f} = (1-\varphi_2)\left\{1 - \varphi_1 + \varphi_1\frac{(\rho c_p)_{s_1}}{(\rho c_p)_f}\right\} + \varphi_2\frac{(\rho c_p)_{s_2}}{(\rho c_p)_f},$$

$$\mu_{hnf} = \frac{\mu_f}{(1-\varphi_1)^{2.5}(1-\varphi_2)^{2.5}},$$

$$\lambda_{hnf} = \frac{\lambda_f}{(1-\varphi_1)^{2.5}(1-\varphi_2)^{2.5}},$$

$$\frac{\sigma_{hnf}}{\sigma_{bf}} = \frac{\sigma_{s_2} + 2\sigma_{bf} - 2\varphi_2(\sigma_{bf} - \sigma_{s_2})}{\sigma_{s_2} + 2\sigma_{bf} + \varphi_2(\sigma_{bf} - \sigma_{s_2})},$$

$$\frac{\sigma_{bf}}{\sigma_f} = \frac{\sigma_{s_1} + 2\sigma_f - 2\varphi_1(\sigma_f - \sigma_{s_1})}{\sigma_{s_1} + 2\sigma_f + \varphi_1(\sigma_f - \sigma_{s_1})},$$

$$\frac{k_{hnf}}{k_{bf}} = \frac{k_{s_2} + 2k_{bf} - 2\varphi_2(k_{bf} - k_{s_2})}{k_{s_2} + 2k_{bf} + \varphi_2(k_{bf} - k_{s_2})},$$

$$\frac{k_{bf}}{k_f} = \frac{k_{s_1} + 2k_f - 2\varphi_1(k_f - k_{s_1})}{k_{s_1} + 2k_f + \varphi_1(k_f - k_{s_1})},$$

where ρ, k, σ, φ_1, φ_2 and c_p, respectively, are density, thermal conductivity, electrical conductivity, volume fractions and specific heat. The subscripts *f*, *hnf*, *nf* stand for fluid, hybrid nanofluid and nanofluid. Further, s_1 stand for Cu and s_2 for Al_2O_3.

Thermophysical properties of both nano-particles (Cu,Al_2O_3) and micropolar fluid (blood) are given in table 1.

3. Numerical method

FEM is a powerful technique and has been successfully implemented to coupled complex and nonlinear problems in computational heat and mass transfer in the recent works [30–35]. For FEM environment, the governing nonlinear coupled problems (7)–(9) are written in residual forms. The residual form are used to construct weighted residual integrals, which are transformed into a weak form by integrating second order linear terms The Galerkin approximations are used to construct elements of local stiffness matrices. Assembly process is carried out to obtained the global stiffness matrix. As problems (7)–(9) are nonlinear due to which the local stiffness matrices and hence global stiffness matrix involve unknown nodal values. The Picard process is implemented to linearize the system of algebraic equations which are solved iteratively under tolerance 10^{-5}. Convergence is ensured and mesh-free analysis is carried out.

Table 1. Values of thermo-physical properties.

Physical property	Blood	Cu	Al_2O_3
$\rho/(\mathrm{kg\ m^{-3}})$	1060	8933	3970
$\mathrm{cp}/(\mathrm{J\ kg^{-1}\ K^{-1}})$	3770	385	765
$\mathrm{k}/(\mathrm{W\ m^{-1}\ K^{-1}})$	0.492	401	40
φ	0.00	0.05	0.15
$\sigma/(\mathrm{s\ m^{-1}})$	4.3×10^{-5}	59.6×10^{6}	35×10^{6}

Table 2. Validation of present results with the results published by Mahdy. [36] and Das *et al* [37] of $-\theta'(0)$ for different Pr when $Ha = C = Ec = \varphi_1 = 0$ and $\varphi_2 = 0$.

Pr	[36]	[37]	Present study
0.72	0.808 68	0.808 76	0.744 54
1.00	1.000 00	1.000 00	0.911 93
3.00	1.923 68	1.923 57	1.815 48
7.00	3.072 24	3.073 14	2.967 45
10.0	3.720 67	3.720 55	3.615 34

4. Results and discussion

Highly nonlinear and complex coupled governing mathematical problems (developed from laws of conservation of mass, linear momentum, angular momentum and energy) are solved by FEM. The developed computer code is tested and verified by comparing the results with the available benchmark. After convergence and grid independent analysis, the macroscopic velocity, microscopic velocity and temperature field are investigated versus parametric variation.

Validation: In order to validate our computational data, we have compared the results with the results of already published benchmark by Mahdy [36] and Das *et al* [37] for different values of Pr and numerical values are recorded in the present table 2. The validation in table 2 shows that results have good agreement with the already published work.

Macro-motion and parametric study: Parameter K represents the dimensionless form of vortex viscosity. The impact of vortex viscosity on macro-motion of nano-micropolar fluid and hybrid nano-micropolar fluid for $n = 0$ are examined and displayed in figure 2. Note that $n = 0$ is the case when micro-motion vanishes at the solid boundary. Figure 2 reveal that macro-velocity of nano-polymeric and hybrid nano-micropolar

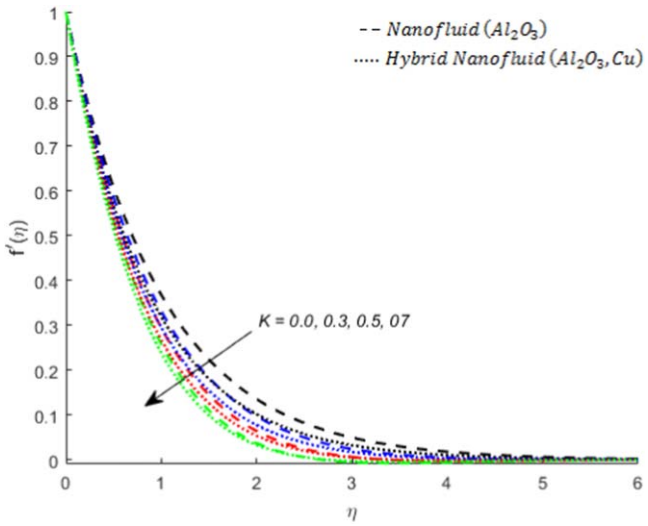

Figure 2. Macro-velocity variation versus K when $n = 0$ and $Ha = 0.3$.

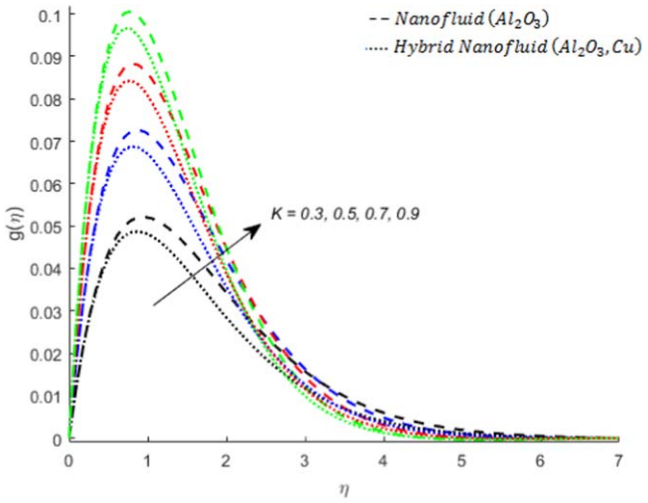

Figure 3. Micro-velocity variation versus K when $n = 0$ and $Ha = 0.3$.

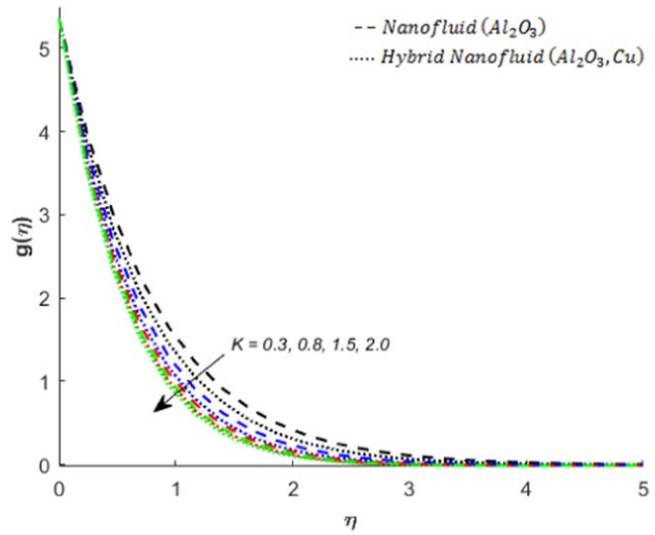

Figure 4. Micro-velocity variation versus K when $n = 0.5$ and $Ha = 0.3$.

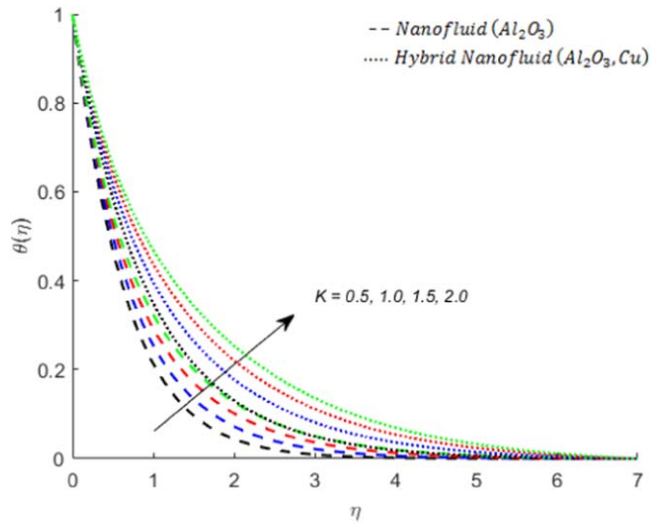

Figure 5. Temperature curve for different values of K when $Pr = 2.36$ and $C = 0.5$.

fluid decreases when vortex viscosity is increased. Figure 2 also demonstrate that wall momentum in hybrid nano-micropolar fluid. Momentum boundary layer thickness for nano-micropolar fluid is greater than the momentum boundary layer thickness for hybrid nano-micropolar fluid.

Micro-motion and parametric study: The angular velocity of nano-micropolar fluid and hybrid nano-micropolar fluid for various values of vortex viscosity are displayed in figures 3 and 4. During numerical computations for angular velocity versus vortex viscosity, it is found that micro-motion slows down when vortex viscosity is increased for $n = 0.5$. However, monotonic behavior for micro-motion of nano-micropolar and hybrid nano-micropolar fluid is observed. Figure 4 also predicts that nano-micropolar fluid rotates faster than the hybrid nano-micropolar fluid.

Temperature profiles for nano-micropolar fluid and hybrid nano-micropolar fluid: Effect of Vortex viscosity on temperature is displayed in figure 5. It is predicted that by increasing vortex viscosity temperature of fluid decreases. The effects of Prandtl and Hartmann numbers on temperature are investigated through numerical experiments. The temperature has a decreasing trend under an increase in the Prandtl number. However, temperature increases when the intensity of the magnetic field is increased. This is shown by figures 6 and 7. It is also observed that the temperature of nano-micropolar fluid is less than the temperature of hybrid nano-micropolar fluid. Figure 8 display the effect of dimensionless material parameter C on dimensionless temperature $\theta(\eta)$. This figure depicts that by increase in dimensionless material parameter temperature of the micropolar fluid increases. The effect of Eckert number is observed in figure 9. A substantial rise in temperature by increasing Eckert number (as a rise in kinetic energy of the micropolar fluid) is noted and displayed in figure 9.

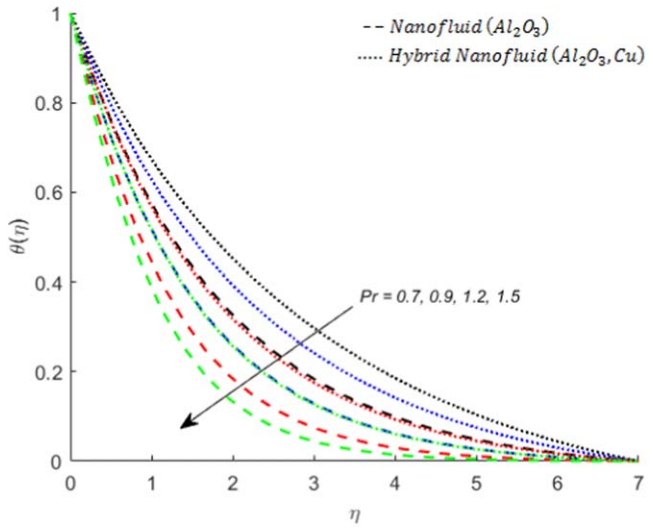

Figure 6. Temperature curves for different values of *Pr*when $K = 0.5$, $Ec = 0.001$, $Re = 15$, $C = 0.5$ and $Ha = 0.3$.

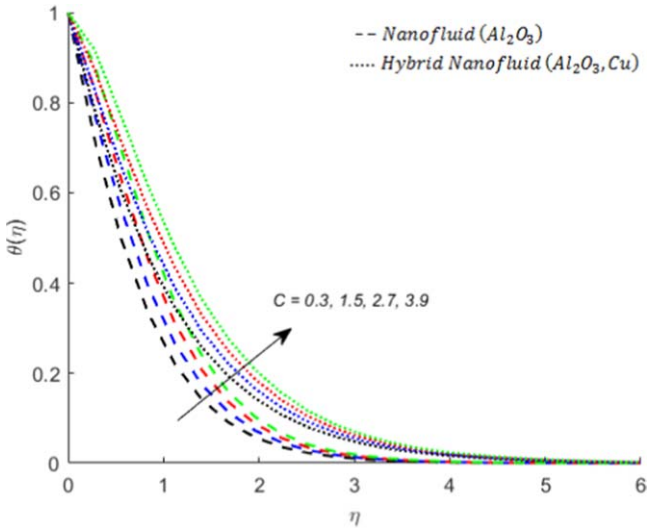

Figure 8. Temperature curves for different values of C when $Pr = 2.36$, $Ec = 0.001$, $Re = 15$, $K = 0.5$ and $Ha = 0.3$.

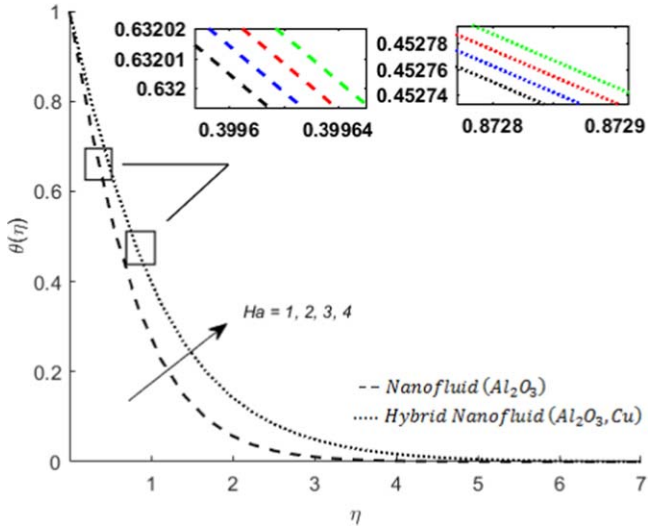

Figure 7. Temperature curves for different values of *Ha* when $Pr = 2.36$, $Ec = 0.001$, $Re = 15$, $K = 0.5$ and $C = 0.5$.

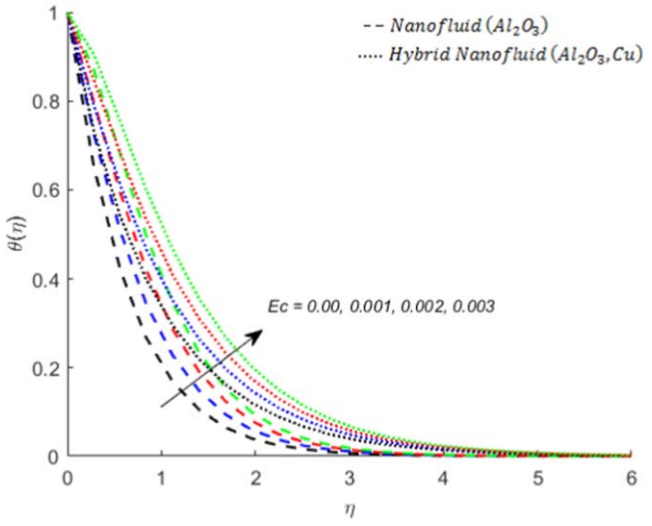

Figure 9. Temperature curves for different values of *Ec* when $Pr = 2.36$, $K = 0.5$, $Re = 15$, $C = 0.5$ and $Ha = 0.3$.

Wall shear stress, wall coupled stress and wall heat flux: Numerical values of wall shear stress, wall coupled stress and wall heat flux versus important physical parameters are computed and displayed in table 3. The underlying physics for shear stress, coupled stress and heat flux is explained as follows.

Wall shear stress versus parametric variation: Wall shear stress for nano-micropolar fluid and hybrid nano-micropolar fluid are investigated versus *Pr*, *n* and *K* and the noted observations are displayed in table 3. This table reflects that the wall (stretching surface) experiences shear stress which increases when vortex viscosity parameter, Prandtl number and parameter *n* are increased. During numerical experiments, it is found that wall shear stress for hybrid nano-micropolar fluid is greater than the wall shear stress for nano-micropolar fluid. It is also observed that wall shear stress (for the case when micro-structures are unable to rotate at the wall) is less than the wall shear stress for the case when micro-structures are able to rotate at the surface of the solid body.

Wall coupled stress and parametric variation: The wall coupled stress is computed versus various values of *Pr* , *K* and *n*. The computed behaviors of wall coupled stress are also displayed in table 3. From these displayed values, it can be observed that coupled stress increases when vortex viscosity parameter, Prandtl number and *n* are increased. Table 3 also demonstrates that wall coupled stress for the case of hybrid nano micropolar fluid is greater than the wall coupled stress for the case of nano micropolar fluid is greater than the wall coupled stress for the case of nano micropolar fluid. Table 3 also predicts that wall coupled stress (for the case when micro-structures are able to rotate at the solid surface) is greater than the wall coupled stress for the case when micro-structures are unable to rotate at the solid surface.

Table 3. The behavior of wall shear stress, wall coupled stress and wall heat flux for nanofluid and hybrid nanofluid when $Ha = 0.3$, $Pr = 2.36$, $C = 0.5$, $Re = 15$, $K = 0.5$ and $Ec = 0.001$.

		Nanofluid			Hybrid nanofluid		
		$-(Re)^{-0.5}C_f$	$-(Re)^{-0.5}C_g$	$-(Re)^{0.5}Nu$	$(Re)^{-0.5}C_f$	$-(Re)^{-0.5}C_g$	$(Re)^{0.5}Nu$
	0.7	1.967 129 903	7.579 695 320	0.612 986 121	1.389 475 899	5.429 683 771	0.677 613 981
Pr	0.9	1.967 129 903	7.579 695 320	0.715 916 332	1.389 475 899	5.429 683 771	0.787 152 309
	1.2	1.967 129 903	7.579 695 320	0.851 878 696	1.389 475 899	5.429 683 771	0.939 402 951
	1.5.	1.967 129 903	7.579 695 320	0.970 202 247	1.389 475 899	5.429 683 771	1.077 755 475
	0.0	1.695 197 668	0.267 821 8395	1.717 527 300	1.253 854 437	0.183 610 741	1.961 724 961
n	0.5	1.967 115 476	7.579 660 0240	1.244 544 545	1.389 475 899	5.429 683 771	1.410 794 148
	1.0	2.257 221 951	15.116 860 301	0.118 850 895	1.534 425 764	10.868 181 143	0.174 750 454
				$n = 0.5$			
	0.0	1.116 551 695	4.984 828 347	1.412 455 287	0.845 883 547	3.776 366 469	1.551 623 783
K	0.8	2.427 641 661	9.040 594 039	1.193 786 032	1.682 611 097	6.383 817 234	1.375 056 230
	1.5	3.364 413 846	12.343 846 088	1.134 197 585	2.283 628 846	8.560 773 722	1.342 643 842
	2.0	3.947 586 255	14.656 566 568	1.112 649 031	2.661 480 053	10.092 277 06	1.335 557 594
				$n = 0$			
	0.5	1.896 726 154	0.305 409 544	1.704 822 807	1.375 964 797	0.206 398 719	1.925 985 506
K	1.0	2.906 938 288	0.613 401 979	1.620 697 870	2.037 898 563	0.410 905 2189	1.809 311 745
	1.5	4.037 389 326	0.932 532 817	1.546 092 285	2.781 046 812	0.622 338 5361	1.707 299 305
	2.0	5.230 850 435	1.230 850 435	1.485 963 401	3.568 901 898	0.837 481 3711	1.627 759 457

Wall heat flux and parametric variation: Wall heat flux for nano-micropolar fluid and hybrid nano-micropolar fluid versus variation of Pr, n and K are displayed in table 3. Wall heat flux speeds up when Pr increased. This observation is for both types of mixtures (nano-polymeric and hybrid nano-polymeric mixtures). However, wall heat flux slows down when K and n is increased. The wall heat flux for the hybrid nano-micropolar fluid is greater than the wall heat flux for the case of nano-micropolar fluid. It also noted that for $n = 0$ (when micro-structures are unable to rotate at the solid surface) less than the wall heat flux when $n = 0.5$ (the case when micro-structures are able to rotate at the solid surface).

5. Final remarks

Mathematical models for nano and hybrid nano-particles are modeled which result in coupled nonlinear and complex mathematical relations in the form of boundary value problems. To capture the underlying physics, solutions of modeled problems are computed via indigenous finite element code. The significant information obtained from numerical experiments are summarized below:

- The simultaneous dispersion of Cu and Al_2O_3 results in an optimized improvement in the thermal performance in comparison of dispersion of single kind of nanoparticles say Cu.
- The vortex viscosity and spin gradient viscosity both have significant effects on temperature and an increase in a vortex and spin gradient viscosities results in a significant decrease in temperature. It is also noted that impact of vortex and spin gradient viscosities on the temperature of a micropolar mixture containing only copper particles is less than the impact of the vortex and spin gradient viscosities on the temperature of a micropolar mixture containing Cu and Al_2O_3.
- The monotonic behavior of angular velocity versus vortex viscosity is noted.
- Optimal heat transfer is observed when simultaneous dispersion of Cu and Al_2O_3 is studied. Thus optimized thermal performances achieved when Cu and Al_2O_3 are simultaneously dispersed.

Acknowledgments

Dr. Salman Saleem extends his appreciation to the deanship of Scientific Research at King Kahlid University for funding this work through general research groups program under grant No. G.R.P-13-41.

ORCID iDs

M Nawaz https://orcid.org/0000-0003-3914-7045
Salman Saleem https://orcid.org/0000-0001-6217-3626

References

[1] Choi S U S 1995 Enhancing thermal conductivity of fluids with nanoparticles *Developments and Applications of Non-*

Newtonian Flows vol 66 ed D A Siginer and H P Wang (New York: ASME) pp 99–105
[2] Dogonchi A S, Waqas M, Seyyedi S M, Hashemi-Tilehnoee M and Ganji D D 2019 CVFEM analysis for Fe_3O_4–H_2O nanofluid in an annulus subject to thermal radiation *Int. J. Heat Mass Transfer* **132** 473–83
[3] Dogonchi A S and Hashim 2019 Heat transfer by natural convection of Fe_3O_4-water nanofluid in an annulus between a wavy circular cylinder and a rhombus *Int. J. Heat Mass Transfer* **130** 320–32
[4] Sheikholeslami M, Shehzad S A, Li Z and Shafee A 2018 Numerical modeling for alumina nanofluid magnetohydrodynamic convective heat transfer in a permeable medium using Darcy law *Int. J. Heat Mass Transfer* **127** 614–22
[5] Sheikholeslami M and Rokni H B 2018 Numerical simulation for impact of Coulomb force on nanofluid heat transfer in a porous enclosure in presence of thermal radiation *Int J. Heat Mass Transfer* **118** 823–31
[6] Sheikholeslami M and Ghasemi A 2018 Solidification heat transfer of nanofluid in existence of thermal radiation by means of FEM *Int. J. Heat Mass Transfer* **123** 418–31
[7] Sheikholeslami M, Haq R, Shafee A, Li Z, Elarakig Y G and Tlili I 2019 Heat transfer simulation of heat storage unit with nanoparticles and fins through a heat exchanger *Int. J. Heat Mass Transfer* **135** 470–8
[8] Sheikholeslami M, Zareei A, Jafaryar M, Shafee A, Li Z, Smidah A and Tlili I 2019 Heat transfer simulation during charging of nanoparticle enhanced PCM within a channel *Physica* A **525** 557–65
[9] Sheikholeslami M, Jafaryar M, Saleem S, Li Z, Shafee A and Jiang Y 2018 Nanofluid heat transfer augmentation and exergy loss inside a pipe equipped with innovative turbulators *Int. J. Heat Mass Transfer* **126** 156–63
[10] Safaei M R, Ranjbarzadeh R, Hajizadeh A, Bahiraei M and Afrand M 2018 Mesoscopic investigation for alumina nanofluid heat transfer in permeable medium influenced by Lorentz forces *Int. J. Refrig.* **349** 839–58
[11] Safaei M R, Hajizadeh A, Afrand M, Qi C, Yarmand H, Bint N W and Zulkifli M 2019 Evaluating the effect of temperature and concentration on the thermal conductivity of ZnO-TiO_2/EG hybrid nanofluid using artificial neural network and curve fitting on experimental data *Physica* A **519** 209–16
[12] Nadeem S, Abbas N and Khan A U 2018 Characteristics of three dimensional stagnation point flow of Hybrid nanofluid past a circular cylinder *Results Phys.* **8** 829–35
[13] Nadeem S, Hayat T and Khan A U 2019 Numerical study on 3D rotating hybrid SWCNT-MWCNT flow over a convectively heated stretching surface with heat generation/absorption *Phys. Scr.* **94** 075202
[14] Iqbal Z, Akbar N S, Azhar E and Maraj E N 2018 Performance of hybrid nanofluid (Cu-CuO/water) on MHD rotating transport in oscillating vertical channel inspired by Hall current and thermal radiation *Alexandria Eng. J.* **57** 1943–54
[15] Nadeem S and Abbas N 2019 On both MHD and slip effect in micro-polar hybrid nano-fluid past a circular cylinder under stagnation point region *Can. J. Phys.* **97** 392–9
[16] Sheikholeslami M, Mehryan S A M, Shafee A and Sheremet M A 2019 Variable magnetic forces impact on magnetizable hybrid nanofluid heat transfer through a circular cavity *J. Mol. Liquids* **277** 388–96
[17] Das S, Jana R N and Makinde O D 2017 MHD Flow of Cu-Al_2O_3/water hybrid nanofluid in porous channel: analysis of entropy generation *Defect Diffus. Forum* **377** 42–61
[18] Olatundun A T and Makinde O D 2017 Analysis of blasius flow of hybrid nanofluids over a convectively heated surface *Defect Diffus. Forum* **377** 29–41
[19] Makinde O D, Kumar K G, Manjunatha S and Gireesha B J 2017 Effect of nonlinear thermal radiation on mhd boundary layer flow and melting heat transfer of micro-polar fluid over a stretching surface with fluid particles suspension *Defect Diffus. Forum* **378** 125–36
[20] Sheikholeslami M, Mustafa M T and Ganji D D 2016 Effect of Lorentz forces on forced-convection nanofluid flow over a stretched surface *Particuology* **26** 108-13
[21] Saleem S, Nadeem S, Rashidi M M and Raju C S K 2019 An optimal analysis of radiated nanomaterial flow with viscous dissipation and heat source *Microsyst. Technol.* **25** 683–9
[22] Sadiq M A, Ullah Khan A, Saleem S and Nadeem S 2019 Numerical simulation of oscillatory oblique stagnation point flow of a magneto micropolar nanofluid *RSC Adv.* **9** 4751–64
[23] Eringen A C 1966 Theory of micropolar fluids *J. Math. Mech.* **16** 1–16
[24] Hayat T, Nawaz M and Obaidat S 2011 Axisymmetric magnetohydrodynamic flow of a micropolar fluid between unsteady stretching surfaces *Appl. Math. Mech.* **32** 361–74
[25] Hayat T, Nawaz M and Hendi A A 2011 Flow of magnetohydrodynamic micropolar fluid between the radially stretching sheets *Z. Naturforsch.* A **66** 53–60
[26] Hayat T, Nawaz M and Obaidat S 2011 Heat transfer analysis on axisymmetric MHD flow of a micropolar fluid between radially stretching sheets *J. Mech.* **27** 607–17
[27] Hayat T, Nawaz M, Hendi A A and Asghar S 2011 MHD squeezing flow of micropolar fluid between parallel disks *J. Fluid Eng.* **133** 111206
[28] Yasushi I D O 2005 Basic equations and constitutive equations of Micropolar magnetic field with E-B Analogy and the abraham expression of electromagnetic momentum *JSME, Int. J. Ser.* B **48** 488–93
[29] Ahmad K, Ishak A and Nazar R 2013 Micropolar fluid flow and heat transfer over a nonlinearly stretching plate with viscous dissipation *Math. Problems Eng.* **2013** 5
[30] Nawaz M, Rana S, Qureshi I H and Hayat T 2018 Three-dimensional heat transfer in the mixture of nano-particles and micropolar MHD plasma with Hall and ion slip effects *AIP Adv.* **8** 105109105109–17
[31] Nawaz M, Rana S and Qureshi I H 2018 Computational fluid dynamic simulations for dispersion of nano-particles in a magnetohydrodynamic liquid: a Galerkin finite element method *RSC Adv.* **8** 38324–35
[32] Nawaz M and Zubair T 2017 Finite element study of three dimensional radiative nano-plasma flow subject to Hall and ion slip currents *Results Phys.* **7** 411–22
[33] Qureshi I H, Nawaz M and Shahzad A 2019 Numerical study of dispersion of nano-particles in magnetohydrodynamic liquid with Hall and ion slip currents *AIP Adv.* **9** 025219
[34] Qureshi I H, Nawaz M, Rana S and Zubair T 2018 Galerkin finite element study on the effects of variable thermal conductivity and variable mass diffusion conductance on heat and mass transfer *Commun. Theor. Phys.* 70
[35] Nawaz M, Arif U and Qureshi I H 2019 Impact of temperature dependent diccusion coefficients on heat and mass transport in viscoelastic liquid using generalized Fourier theory *Phys. Scr.* (https://doi.org/10.1088/1402-4896/ab1cec)
[36] Mahdy A 2012 Unsteady mixed convection boundary layer flow and heat transfer of nanofluids due to stretching sheet *Nucl. Eng. Des.* **249** 248–55
[37] Das S, Chakraborty S, Jana R N and Makinde O D 2015 Entropy analysis of unsteady magneto-nanofluid flow past accelerating stretching sheet with convective boundary condition *Appl. Math. Mech.* **36** 1593–610